INFECTION AND IMMUNITY, Mar. 2002, p. 1310–1318 Vol. 70, No. 3
0019-9567/02/$04.00+0 DOI: 10.1128/IAI.70.3.1310–1318.2002

Retrieving Biological Activity from LukF-PV Mutants Combined with Different S Components Implies Compatibility between the Stem Domains of These Staphylococcal Bicomponent Leucotoxins

S. Werner,[1] D. A. Colin,[1] M. Coraiola,[2] G. Menestrina,[2] H. Monteil,[1] and G. Prévost[1]*

Laboratoire de Physiopathologie et d'Antibiologie des Infections Bactériennes Emergentes et Nosocomiales, Institut de Bactériologie de la Faculté de Médecine, Université Louis Pasteur, F-67000 Strasbourg, France,[1] *and CNR-ITC Centro Fisica Stati Aggregati, I-38050 Povo Trento, Italy*[2]

Received 10 July 2001/Returned for modification 25 October 2001/Accepted 11 December 2001

Bicomponent leucotoxins, such as Panton-Valentine leucocidin, are composed of two classes of proteins, a class S protein such as LukS-PV, which bears the cell membrane binding function, and a class F protein such as LukF-PV, which interacts to form a bipartite hexameric pore. These leucotoxins induce cell activation, linked to a Ca^{2+} influx, and pore formation as two consecutive and independently inhibitable events. Knowledge of the LukF-PV monomer structure has indicated that the stem domain is folded into three antiparallel β-strands in the water-soluble form and has to refold into a transmembrane β-hairpin during pore formation. To investigate the requirements for the cooperative assembly of the stems of the S and F components to produce biological activity, we introduced multiple deletions or single point mutations into the stem domains of LukF-PV and HlgB. While the binding of the mutated proteins was weakly dependent on these changes, Ca^{2+} influx and pore formation were affected differently, confirming that they are independent events. Ca^{2+} entry into human polymorphonuclear cells requires oligomerization and may follow the formation of a prepore. The activity of some of the LukF-PV mutants, carrying the shorter deletions, was actually improved. This demonstrated that a crucial event in the action of these toxins is the transition of the prefolded stem into the extended β-hairpins and that this step may be facilitated by small deletions that remove some of the interactions stabilizing the folded structure.

Pore-forming toxins, rich in β-sheet structures, include a variety of molecules such as staphylococcal alpha-toxin, aerolysin, anthrax protective antigen, perfringolysin O, and staphylococcal bicomponent leucotoxins (1, 9, 14). These last molecules comprise six class S proteins, which bind first to the membrane, and five class F proteins, whose consecutive interaction induces a rapid activation of Ca^{2+} channels (21). Their oligomerization leads, after a delay (23), to the formation of hetero-hexameric pores with an equimolar ratio of class S and F proteins (5, 17), which are permeable to monovalent cations. Activation and pore formation were demonstrated to be independent by their specific inhibition (23) and their functional discoupling via mutagenesis (2).

The structure of the closely related alpha-toxin pore (22) revealed a heptameric mushroom-shaped structure where each monomer participates with one β-hairpin to the assembly of the transmembrane region, called the stem. The structural characterization of HlgB (18) and LukF-PV (19) monomers clarified that, in the soluble proteins, the stem domain is folded as three antiparallel β-strands stacked to a β-sandwich core of 12 β-strands. Based on the alpha-toxin model and on several observations (5, 21) a hexameric pore is strongly suggested for leucotoxins (19). It proceeds from a series of rearrangements essentially focused on the stem domain, occurring from the binding of monomers to membrane ligands, the oligomerization of monomers, and the insertion of six β-hairpins enabling the formation of a β-barrel with a lumen of about 22 Å diameter (2).

Despite being related in structure, alpha-toxin and leucotoxins do not exactly target the same cells and do not compete on rabbit erythrocytes (RRBC); also, different S components do not always compete at the same sites (8). The sensitivity of blood cells varies according to the S/F couple. Panton-Valentine leucocidin (LukS-PV plus LukF-PV or PVL) and gamma-hemolysins (HlgA plus HlgB and HlgC plus HlgB) are active on polymorphonuclear cells (PMNs), monocytes, and macrophages of rabbit and human origin, but HlgA plus HlgB can also lyse some human T lymphocytes and erythrocytes (5, 17, 20). Moreover, couples such as one PVL component and one gamma-hemolysin heterologous component are active (10, 20). Since several members of the bicomponent family can be produced by a single bacterial isolate, one might keep this possibility in mind when considering the true contribution of a given couple to virulence.

It has been suggested that leucotoxins and related toxins are derived from a common ancestor (15). Up to now, it was not known whether a molecular compatibility between S and F β-hairpins may influence the biological activity of leucotoxins. In order to clarify the functional role of F components, especially in the formation of the pore, a series of deletions were generated in the stem domain of LukF-PV and HlgB. Their ability to open Ca^{2+} channels and to form pores in combination with class S proteins was determined to define residues important for functional compatibility of the β-hairpins.

* Corresponding author. Mailing address: Laboratoire de Physiopatholgie et d'Antibiologie des Infections Bacteriennes Emergentes et Nosocomiales–-EA 3432. Institut de Bacteriologie, Universite Louis Pasteur, 3 rue Koeberle, F-67000 Strasbourg, France. Phone: 33-3-90-24-37-57. Fax: 33-3-88-25-11-13. E-mail: gilles.prevost@medecine.u-strasbg.fr.

MATERIALS AND METHODS

Bacterial strains and vectors. *Escherichia coli* XL1 Blue cells (*recA1 endA1 gyrA96 thi1 hsdR17 supE44 relA1 lac* [F′ *proAB lacI*^{q} *Z*ΔM15 Tn*10*] [*tet*^{r}]) (Stratagene, Amsterdam, The Netherlands) were used as recipient cells after site-directed mutagenesis of recombinant plasmids. E. coli BL21 [F$^-$ *ompT hsdS* (*rB*$^-$ *mB*$^-$) *gal*] was used for overexpression of the pGEX-6P-1 glutathione *S*-transferase (GST)-fusioned leucotoxins as recommended by the manufacturer (Pharmacia, Uppsala, Sweden) (2).

Chemical reagents. Lipids used were phosphatidylcholine (PC) and lissamine-rhodamine phosphatidylethanolamine (LR-PE), both purchased from Avanti Polar Lipids (Webster, Tex.), and cholesterol (Cho) by Fluka. Other reagents were calcein, EDTA, Sephadex (Sigma), sodium dodecyl sulfate (SDS) (Pierce), and Triton X-100 (Merck).

Construction of LukF-PV and HlgB mutants in *E. coli*. Of the 10 LukF-PV mutants used in this work, four of them (i.e., LukF-PV G130D, G131D, ΔS125-L128, and ΔI124-S129) were already described (2), though they were evaluated only in combination with LukS-PV. The other five LukF-PV mutants (i.e., LukF-PV S129A, ΔN123-G127, ΔI124-N126, ΔS125-G127, and ΔG127-S129) and HlgB G130D were prepared new. All mutants were constructed using the QuickChange mutagenesis kit (Stratagene) and dedicated oligonucleotides as described previously (2). Proteins were purified by affinity chromatography on glutathione-Sepharose 4B followed by cation-exchange fast-performance liquid chromatography (2, 10), after removal of the GST tag with Precision Protease (Amersham-Pharmacia), and they were controlled for homogeneity by radial gel immunoprecipitation and SDS-polyacrylamide gel electrophoresis (SDS-PAGE) before being stored at −80°C. LukF-PV S27C and HlgB S27C, two functional mutated proteins, were labeled with fluorescein 5-maleimide (Molecular Probes, Leiden, The Netherlands) (2).

Human PMNs and flow cytometry measurements. Human PMNs from healthy donors were purified from buffy coats as previously reported (2) and resuspended at 5×10^5 cells/ml. Flow cytometry measurements from 3,000 PMNs were performed using a FacSort cytometer (Becton Dickinson, Le Pont de Claix, France) equipped with an argon laser tuned at 488 nm (16). Fluo-3 fluorescence (Molecular Probes) for Ca^{2+} entry and ethidium fluorescence were acquired with Lysis II software (Becton Dickinson) as previously mentioned (2). Results from at least four different donors were averaged and expressed as percentages of a control of human PMNs treated with the wild-type (wt) PVL. Base-level values were obtained for each series of data from a control without toxin and were systematically subtracted from the other assays.

LukF-PV, whose dissociation constant ($k_{D[F]}$) for the PMN membrane-bound LukS-PV is 2.5 nM (7), and mutants were applied at 40 nM concentrations together with 1 nM LukS-PV, 2 nM HlgA, or 1 nM HlgC. HlgB and HlgB G130D were applied at 5 nM because of a lower k_D with LukS-PV ($k_{D[B]} = 0.44$ nM) (7). The dissociation constant of HlgB for the bound HlgA is not known, due to the complex saturation of HlgA (17). HlgB proteins were therefore used also at 5 nM for associations with HlgA or HlgC.

Competition experiments. Competition experiments were performed in the absence of extracellular Ca^{2+} on PMNs previously incubated for 10 min with 1 nM LukS-PV or HlgC, or with 2 nM HlgA. Fluorescein-labeled LukF-PV S27C (20 nM) and increasing concentrations of mutated proteins (from 1 to 1,000 nM) were added 15 min before fluorescence measurement. IC_{50}, the concentration of nonfluorescent competitor needed for 50% fluorescence inhibition, was determined from the best fit of independent triplicates of the residual cell fluorescence (2). $K_{i(app)}$, the apparent inhibition constant, was calculated as $K_{i(app)} = IC_{50}/(1+[F^*]/k_{D[F]})$, where [F*] is the concentration of fluorescent LukF-PV or HlgB S27C and $k_{D[F]}$ is the dissociation constant of LukF-PV (2.5 nM) or HlgB (0.44 nM) for LukS-PV (7).

Determination of pore radii. The radius of pores formed by native and modified leucotoxins was assessed by the relative ability of polyethylene glycol (PEG) molecules of various sizes to protect cells from osmotic leakage if they cannot pass through the pores because their diameter is similar or greater than the lumen. The relative variations of PMN sizes were assessed by measuring the variations of the forward light scatter (FSC) of cells (5×10^5 cells/ml) treated with 1 nM LukS-PV, 40 nM LukF-PV wt or mutants, and 30 mM PEG polymers of different hydrodynamic radii (0.94, 1.2, 1.22, and 1.44 nm). FSC values were collected at 0, 10, 20, and 30 min after toxin application (2).

Hemolytic activities. Hemolytic activities on RRBC or human erythrocytes (HRBC) were determined in microplates as described elsewhere (20). Each well contained a constant concentration of the S protein (65 nM) and 1:2 serial dilutions of the F protein starting from 700 nM. Critical hemolytic concentrations of F proteins were defined as those still able to achieve hemolysis, as measured by the absorbance at 410 nm compared to that of the control with 0.5% (wt/vol) saponin.

Permeabilization of lipid vesicles by leucotoxins. For calcein release experiments, large unilamellar lipid vesicles (LUV) were prepared by extrusion of 4 mg of PC/ml and Cho at a 1:1 molar ratio, as described previously (24). LUV were washed on Sephadex G-50 medium preequilibrated with 50 mM NaCl, 0.1 mM EDTA, 20 mM Tris-HCl, pH 7.0. Permeabilization was assayed with a fluorescence microplate reader. Each well contained LUV (5 μM lipid) and variable dilutions of leucotoxins (the two components being always at the same concentration) in 200 μl of 20 mM NaCl, 0.1 mM EDTA, 20 mM Tris-HCl, pH 7.0. Maximal protein concentration was 0.05 μM with HlgB plus HlgA, 0.1 μM with HlgB plus HlgC, and up to 4 μM with LukF-PV and its mutants.

Identification of oligomers. Denaturing SDS-PAGE was carried out from human PMN or RRBC preparations at 3×10^7 cells/ml in the EGTA buffer and incubated for 20 min with 30 nM LukS-PV and 600 nM LukF-PV or derivatives. Cells were pelleted for 10 min at $800 \times g$ and resuspended at the initial density with 10 mM Tris-HCl, 10 mM Na_2EDTA, pH 7.5, and then supplemented with 2.0% (wt/vol) SDS, mixed, and loaded on a 4-to-15% (wt/vol) polyacrylamide gel (Mini-Protean II; Bio-Rad) after addition of 30% (vol/vol) loading buffer (25% [vol/vol] glycerol, 62.5 mM Tris-HCl, 0.125% [wt/vol] bromophenol blue, 0.5% [wt/vol] SDS, pH 6.8). Apparent molecular masses were estimated on protein migration with respect to the following molecular weight markers: myosin (212 kDa), α_2-macroglobulin (170 kDa), β-galactosidase (116 kDa), transferrin (76 kDa), glutamate dehydrogenase (53 kDa) (Pharmacia), and LukF-PV (34 kDa). An immunoblot transfer was performed onto nitrocellulose by using a mini Trans-Blot apparatus (Bio-Rad). Oligomers were detected using an Amplified Opti4CN Substrate kit (Bio-Rad) after the application of rabbit affinity-purified specific antibodies (10) followed by rabbit immunoglobulin G coupled to horseradish peroxidase (Sigma). Either anti-S or anti-F antibodies could be used; however, only results obtained with both antibodies are shown (see Fig. 4A).

For oligomers on pure lipid vesicles, LUV comprised of PC-Cho (1:1 molar ratio) and 1% (wt/vol) LR-PE were extruded as above at a 1-mg/ml lipid concentration in 20 mM Tris-HCl, 0.1 mM EDTA, pH 7.0, and then diluted to 0.4 mM lipid and incubated with a 2 μM concentration of each leucotoxin component in 100 μl of the same buffer. After 1 h at 25°C, they were diluted to 1 ml in the above buffer and pelleted at 4°C by 3 h of ultracentrifugation at $400,000 \times g$ in a fixed angle rotor (Beckman TLA-100.2). Measuring the fluorescence of LR-PE, we ascertained that all the lipid was precipitated in this way. Control tubes with the protein, but no vesicles, were included. Pellets were resuspended in 4 μl of 2.5% (wt/vol) SDS and subjected to SDS-PAGE at 10°C in 0.5% (wt/vol) SDS using PhastSystem 8 to 25% (wt/vol) polyacrylamide precast minigels (Pharmacia). Gels were stained as described previously (5). The apparent molecular mass of proteins was estimated using the program Phoretix TotalLab (Hitachi Software). The standards (Pharmacia) included were reduced ferritin (220 kDa), phosphorylase B (94 kDa), albumin (67 kDa), ovalbumin (43 kDa), and carbonic anhydrase (30 kDa).

RESULTS

Competition of mutants of LukF-PV and HlgB on human PMNs. As shown in Table 1, five LukF-PV mutants, G131D, ΔS125-G127, ΔS125-L128, ΔG127-S129, and S129A, had binding properties comparable to that of the wt. Three LukF-PV mutants, ΔN123-G127, ΔI124-N126 and, more markedly, G130D, showed an increased binding. Only one, LukF-PV ΔI124-S129, remarkably lost affinity. The binding of HlgB G130D to LukS-PV, HlgA, or HlgC remained very similar to that of HlgB.

Ca^{2+} entry in human PMNs. Upon addition of leucotoxins to PMNs, fluo-3 fluorescence rapidly reached a maximal value, indicating Ca^{2+} entry (Fig. 1). The percentage of the maximal fluorescence compared to that of the wt and the time necessary to reach it were considered to quantify this action (Table 2). As shown in Table 2 and exemplified in Fig. 1, three categories of mutated proteins could be distinguished.

(i) LukF-PV ΔI124-N126, ΔS125-G127, ΔG127-S129, and S129A had a strong ability to promote Ca^{2+} entry, whatever the S protein combined (Table 2). Kinetics obtained with

TABLE 1. Binding of the mutated LukF-PV and HlgB

Class F protein	Class S protein binding ability (nM)			
	LukS-PV		HlgA IC_{50}	HlgC IC_{50}
	IC_{50}[a]	$K_{i(app)}$[a]		
LukF-PV	21.1 ± 6	2.4 ± 0.7	27.6 ± 8	37.9 ± 9
LukF-PV Gly130Asp	5.5 ± 0.8	0.5 ± 0.1	2.1 ± 0.4	6.9 ± 1
LukF-PV Gly131Asp	21.5 ± 5	2.4 ± 0.6	28.2 ± 4	40.3 ± 8
LukF-PV Ser129Ala	22.4 ± 4	2.6 ± 0.5	30.1 ± 7	40.9 ± 8
LukF-PV ΔAsn123-Gly127	9.8 ± 2	1.1 ± 0.2	12.9 ± 5	19.3 ± 4
LukF-PV ΔIle124-Asn126	10.8 ± 2	1.2 ± 0.2	13.5 ± 5	16.1 ± 5
LukF-PV ΔIle124-Ser129	62.6 ± 8	6.9 ± 0.9	79.7 ± 12	88.4 ± 11
LukF-PV ΔSer125-Gly127	19.1 ± 4	2.1 ± 0.4	26.1 ± 7	30.9 ± 5
LukF-PV ΔSer125-Leu128	16.1 ± 7	1.8 ± 0.8	22.1 ± 9	28.3 ± 8
LukF-PV ΔGly127-Ser129	22.6 ± 6	2.5 ± 0.7	26.4 ± 6	33.7 ± 6
HlgB	4.9 ± 0.5	0.4 ± 0.1	4.5 ± 0.4	1.4 ± 0.2
HlgB Gly130Asp	5.8 ± 0.7	0.5 ± 0.1	7.9 ± 0.9	2.4 ± 0.3

[a] IC_{50} and $K_{i(app)}$ are defined in Materials and Methods.

LukF-PV ΔI124-N126 (Fig. 1), ΔS125-G127, and ΔG127-S129 in combination with HlgC were faster and reached a higher maximum than that obtained with LukF-PV. LukF-PV S129A produced kinetics always identical to LukF-PV.

(ii) LukF-PV Δ78 123-G127 (Fig. 1), ΔS125-L128, G130D, and G131D caused variable Ca^{2+} influxes according to the combined S protein: LukS-PV, HlgA, or HlgC (Table 2). Even at 40 nM, LukF-PV ΔN123-G127, in combination with LukS-PV, induced a lower Ca^{2+} entry than that recorded with only 2 nM LukF-PV (Fig. 1). However, if it was combined with either HlgA or HlgC, Ca^{2+} entry approached that obtained with wt pairs. LukF-PV G131D at 40 nM was as effective as LukF-PV in association with HlgA but was only comparable to 2 nM LukF-PV when combined with either LukS-PV or HlgC. At 40 nM, LukF-PV G130D combined with HlgA or LukS-PV promoted a level of Ca^{2+} entry close to that with 2 nM LukF-

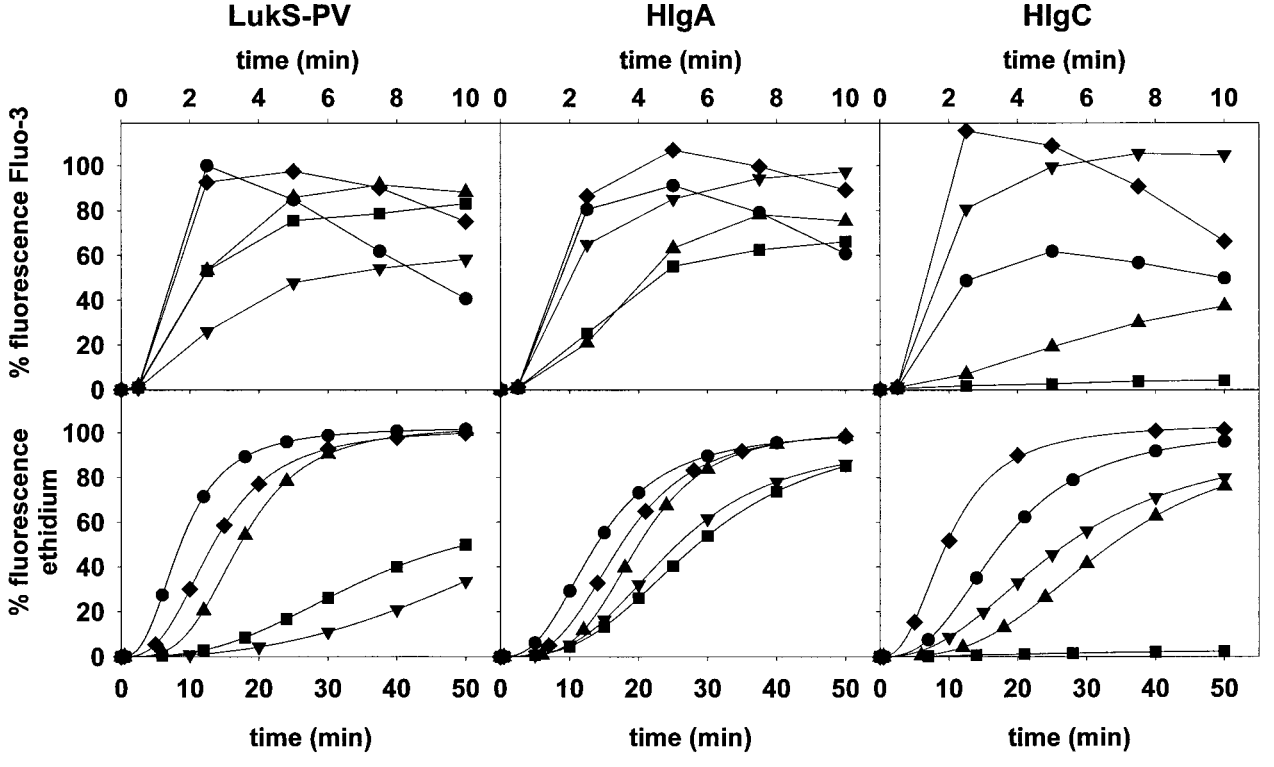

FIG. 1. Flow cytometry evaluation of the kinetics of Ca^{2+} influx (upper panel) and pore formation (lower panel) in PMNs as induced by combinations of one S component with LukF-PV or its mutants. (Upper panel) PMNs, previously loaded with 5 μM Fluo-3, were observed in the presence of 1.1 mM extracellular Ca^{2+}. (Lower panel) PMNs, after incubation with 4 μM ethidium, were observed in the absence of extracellular Ca^{2+}. F components used were LukF-PV (●), LukF-PV 2 nM (▲), LukF-PV ΔN123-G127 (▼), LukF-PV ΔI124-N126 (♦), and LukF-PV G130D (■). Points are means of independent quadruplicates. Error bars are not reported for clarity, but they did not exceed ±8%, except for HlgA+LukF-PV ΔI124-N126 and HlgC+LukF-PV ΔI124-AN126, for which values were up to ±15%.

TABLE 2. Biological activities of mutated LukF-PV and HlgB combined with LukS-PV, HlgA, or HlgC

F protein[c]	S protein activity (time [min])					
	Ca^{2+} entry[a]			Ethidium entry[b]		
	LukS-PV	HlgA	HlgC	LukS-PV	HlgA	HlgC
LukF-PV	100 (2.5)	91 ± 3 (5)	61 ± 7 (5)	8.4 ± 0.4 (1)	5.2 ± 0.2 (2)	4.2 ± 0.3 (4)
LukF-PV (2 nM)	92 ± 2 (7.5)	80 ± 9 (7.5)	36 ± 19 (10)	4.7 ± 0.2 (3)	4.8 ± 0.2 (6)	2.5 ± 0.2 (7)
F Gly130Asp	83 ± 4 (10)	71 ± 10 (10)	0	1.4 ± 0.1 (10)	2.8 ± 0.2 (6)	0
F Gly131Asp	95 ± 3 (5)	91 ± 1 (5)	30 ± 5 (5)	2.6 ± 0.1 (6)	4.9 ± 0.3 (3)	0.8 ± 0.2 (6)
F ΔAsn123-Gly127	56 ± 9 (10)	91 ± 11 (10)	98 ± 21 (7.5)	1.1 ± 0.1 (20)	3.1 ± 0.3 (6)	2.6 ± 0.2 (3)
F ΔIle124-Asn126	96 ± 7 (2.5)	102 ± 17 (5)	109 ± 20 (2.5)	3.4 ± 0.3 (4)	5.1 ± 0.2 (3)	7.0 ± 0.5 (1)
F ΔIle124-Ser129	0	0	0	0	0	0
F ΔSer125-Gly127	99 ± 3 (2.5)	93 ± 3 (5)	96 ± 2 (2.5)	9.7 ± 0.2 (1)	5.0 ± 0.2 (2)	10.2 ± 0.2 (1)
F ΔSer125-Leu128	90 ± 13 (5)	90 ± 4 (5)	92 ± 6 (2.5)	2.7 ± 0.1 (5)	4.8 ± 0.3 (3)	5.6 ± 0.4 (1)
F ΔGly127-Ser129	101 ± 7 (2.5)	89 ± 4 (5)	88 ± 3 (2.5)	4.9 ± 0.4 (2)	4.6 ± 0.2 (2)	7.0 ± 0.4 (1)
F Ser129Ala	97 ± 1 (2.5)	90 ± 2 (5)	64 ± 7 (5)	8.2 ± 0.2 (1)	4.9 ± 0.1 (2)	5.0 ± 0.2 (4)
HlgB	88 ± 5 (5)	89 ± 4 (2.5)	78 ± 6 (2.5)	5.9 ± 0.4 (1)	3.8 ± 0.3 (2)	3.5 ± 0.2 (2)
HlgB (0.5 nM)	44 ± 16 (10)	83 ± 7 (5)	59 ± 12 (7.5)	3.0 ± 0.3 (3)	3 ± 0.4 (2)	3.0 ± 0.2 (3)
HlgB Gly130Asp	85 ± 6 (7.5)	87 ± 2 (5)	30 ± 11 (2.5)	3.5 ± 0.4 (2)	2.9 ± 0.3 (3)	0.9 ± 0.1 (7)

[a] Fluorescence maxima as percentages from control ± standard deviations; time (minutes) necessary to reach the maximal fluorescence is shown in parentheses.
[b] Rate of ethidium entry as a variation of fluorescence/minute; lag time (minutes) before the increase of fluorescence is shown in parentheses.
[c] If not otherwise specified, protein concentrations were as follows: LukS-PV, 1 nM; HlgA, 2 nM; HlgC, 1 nM; LukF-PV as well as all LukF-PV mutants, 40 nM; HlgB and HlgB G130D, 5 nM.

PV, but it had no activity with HlgC. Finally, LukF-PV ΔS125-L128 caused a slightly decreased Ca^{2+} influx with LukS-PV but was as effective as the native protein with HlgA, and even more efficient with HlgC.

HlgB G130D was always less active than HlgB. At a concentration of 5 nM, it was slightly faster than 0.5 nM HlgB when coupled to LukS-PV, comparable to 0.5 nM HlgB in combination with HlgA, and had only a residual activity with HlgC (Table 2).

(iii) One mutant, LukF-PV ΔI124-S129, never induced any Ca^{2+} entry inside the PMNs, whatever the combined class S component.

Ethidium entry in human PMNs. Independently of Ca^{2+} entry (23), leucotoxins can form pores for monovalent cations that can be blocked by 0.2 mM Zn^{2+}. By characterizing pore formation via the lag time preceding ethidium entry and its initial rate (Table 2; Fig. 1), two groups of LukF-PV mutants were defined in comparison to Ca^{2+} entry.

(i) LukF-PV ΔS125-G127, ΔI124-S129, S129A, and HlgB G130D promoted an ethidium entry that was comparable in extent to Ca^{2+} entry (Table 2; Fig. 1).

(ii) To the contrary, LukF-PV ΔN123-G127, ΔI124-N126 (Fig. 1), ΔG127-S129, G130D (Fig. 1), ΔS125-L128, and G131D displayed, at least with one S component, decreases in ethidium entry (compared to wt) that were not correlated to similar decreases of Ca^{2+} intake (Table 2). Such discoupling was observed with all these mutants in association with LukS-PV, whereas for combinations with HlgA, ethidium entry was only discoupled for LukF-PV ΔN123-G127 and G130D. The other combinations with HlgA remained as active as the wt toxin. LukS-PV and HlgC pairs, including LukF-PV G131D, were also discoupled. Significant discoupling in a pair containing HlgC was only observed with LukF-PV ΔN123-G127. Curiously, LukF-PV G130D lost all biological activity in combination with HlgC, whereas HlgB G130D retained some (Table 2). With HlgC, LukF-PV ΔI124-N126 and ΔS125-L128 mutants were more active than the corresponding wt couples either for Ca^{2+} or for ethidium entry (Table 2; Fig. 1).

Determination of radii of pores formed by mutated LukF-PV-S protein couples. A shift of mean FSC toward lower values was observed for all combinations retaining a biological activity with PEG molecules of 1.22 nm radius (Fig. 2). The nonactive combination HlgC plus LukF-PV G130D did not induce a significant shift (Fig. 2C), nor did LukF-PV ΔI124-S129 in combination with any class S proteins (2). Thus, there was a consistent correlation between the absence of permeability to ethidium and that to neutral molecules such as PEG.

Hemolytic activities on RRBC and HRBC. Among bicomponent leucotoxins, HlgA plus HlgB and HlgC plus HlgB are significantly hemolytic against RRBC (5, 20). As some of the mutated proteins showed enhanced biological activities with respect to wt combinations, their hemolytic activities were also tested (Fig. 3). With 65 nM HlgA, a minimal concentration of 384 nM LukF-PV is necessary for a complete hemolysis of RRBC (critical concentration). Interestingly, in the same combination, five deletion mutants, i.e., LukF-PV ΔI124-N126, ΔS125-G127, ΔS125-L128, ΔG127-S129, and ΔN123-G127 induced hemolysis with critical concentrations of 6.8, 14.9, 33.5, 45.8, and 50.0 nM, respectively. In addition, LukF-PV S129A was as effective as the native protein. In combination with HlgC, only LukF-PV ΔG127-S129, ΔS125-G127, and ΔN123-G127 showed limited hemolytic properties on RRBC with critical concentrations of 80, 160, and 160 nM, respectively, whereas none of the mutants had a significant hemolytic activity in combination with LukS-PV. HlgA combined with HlgB was hemolytic at the concentration of 75.6 pM, while HlgB G130D was only hemolytic at 385 pM.

When applied to HRBC, 65 nM HlgA combined with 768 nM LukF-PV, or most of the LukF-PV mutants, did not generate hemolysis. Only HlgA plus LukF-PV ΔS125-G127 (119 nM) was hemolytic. HlgA plus HlgB (0.6 nM) promoted he-

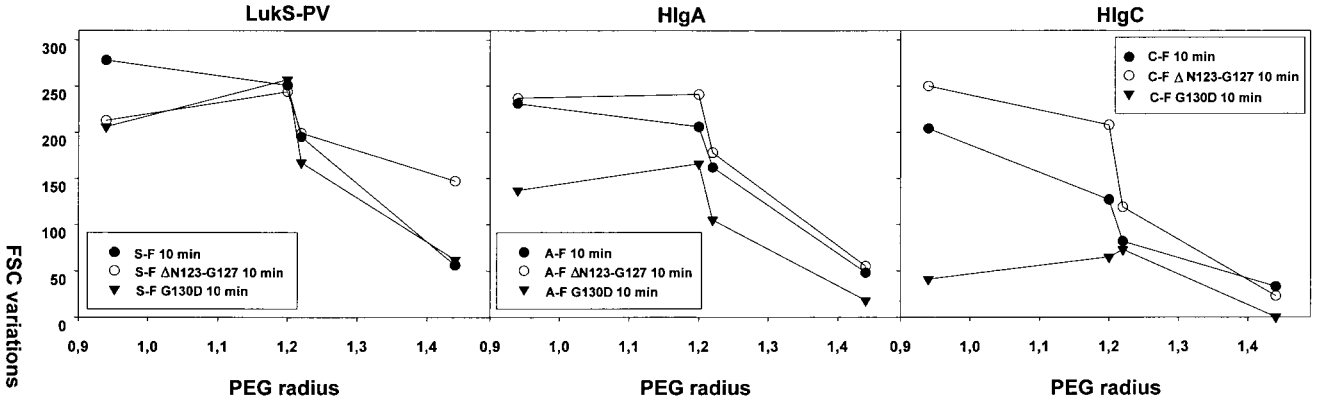

FIG. 2. Illustration of the determination of the radius of pores formed by nine of the different combinations of class S and class F proteins. Permeabilizations were assessed by variations of the mean value of the FSC in the presence of PEG molecules of different hydrodynamic radii. LukF-PV, LukF-PV N123-G127, and LukF-PV G130D were combined with LukS-PV, HlgA, and HlgC. As the FSC values did not increase from 10 to 20 or 30 min after toxin application under the experimental conditions, only the values obtained at 10 min are shown.

molysis of HRBC, but HlgB G130D did it only at 6.2 nM and reached a maximum after 2 h instead of 1 h.

Characterization of oligomers. Typically, alpha-toxin oligomers can be detected from SDS-lysed RRBC (25). A derived method allowed us to detect, on human PMNs, leucotoxin oligomers with an apparent molecular mass comprised between 170 and 200 kDa, compatible with the formation of a hexamer (Fig. 4A). Oligomers were observed with each LukF-PV mutant when combined with either LukS-PV or HlgA or HlgC (data not shown), independently of whether the couple was active or not. In particular, when HlgC was associated to LukF-PV G130D or to LukF-PV G131D, the biological activity was completely abolished for the first couple and the second displayed only a weak Ca^{2+} intake (Fig. 1 and 4).

To the contrary, combinations with HlgA were characterized by low yields of oligomers even when PMNs were permeabilized, maybe because of subsequent proteolytic events (Fig. 4A). The presence of intermediates, or incomplete pores, was also revealed, possibly due to the unspecific, not saturable, binding of HlgA (17).

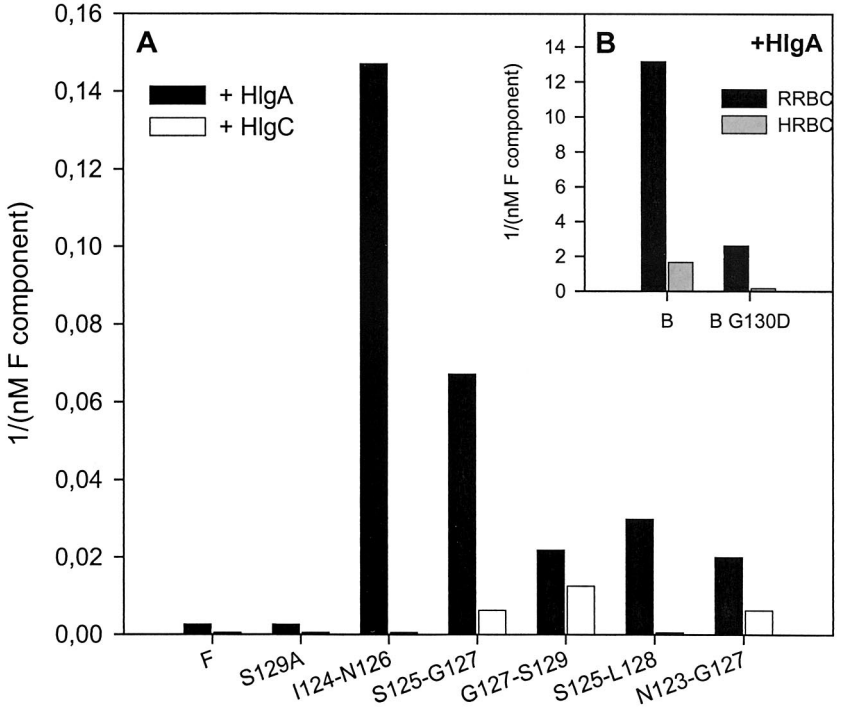

FIG. 3. Hemolytic properties of LukF-PV and HlgB mutants compared to wt controls. (A) Hemolytic activity on RRBC, expressed as 1/critical concentration (nanomolar^{-1}) of the active LukF-PV mutants associated with either HlgA (black) or HlgC (white). Only LukF-PV mutants ΔS125-L128, ΔG127-S129, and ΔN123-G127 are hemolytic with HlgC. (B) Hemolytic activity on RRBC (black) and on HRBC (grey) of HlgB wt and HlgB G130D in association with HlgA.

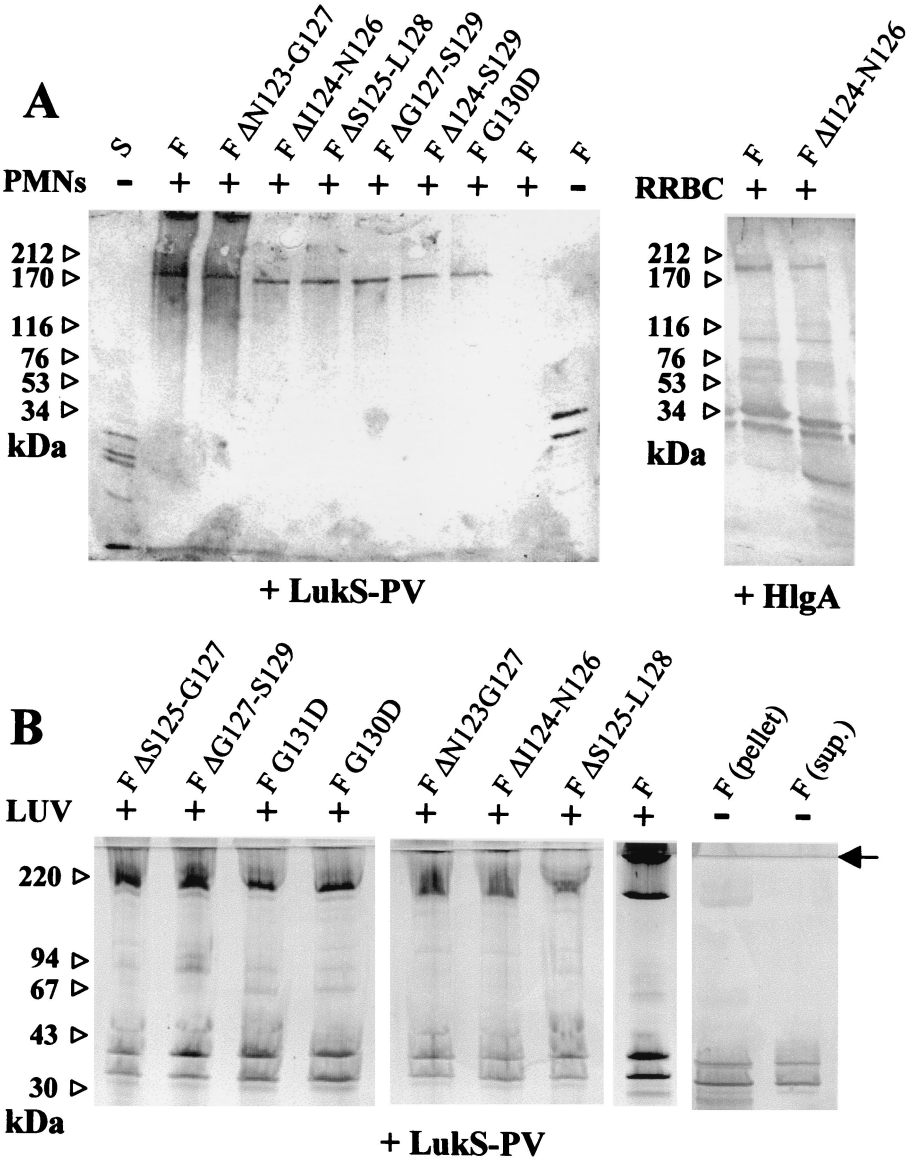

FIG. 4. Characterization of leucotoxin oligomers on different membrane systems. (A) Human PMNs or RRBC (30×10^6 cells/ml) were treated with 60 nM S protein and 600 nM F protein before being submitted to SDS-PAGE, and oligomers were revealed by immunoblotting with both anti-LukS-PV and anti-LukF-PV rabbit polyclonal antibodies. Combinations of LukF-PV or mutants were tested with either LukS-PV or HlgA. Controls of cells with components alone or of components with (+) and without (−) cells are indicated. (B) Assembly of leucotoxin oligomers by native and mutated LukF-PV on model membranes. Leucotoxin oligomers formed by the indicated form of LukF-PV in association with either LukS-PV were detected by SDS-PAGE of the vesicles pelleted after ultracentrifugation. Controls of native leucotoxin without lipids, separated in pellet and supernatant, are included in the left panel. Some streaking appears in the lanes with lipids. The end of the stacking gel is indicated by an arrow. Left lane, molecular standards.

Even if PC-Cho LUV were not permeabilized by any of the combinations including a mutant of LukF-PV or HlgB, a lipid-bound, high-molecular-mass oligomer was observed with many of these couples (Fig. 4B), though never with single components (data not shown). The extent of oligomerization, represented in each lane by the ratio between the intensity of the oligomeric and the monomeric bands, was similar for all couples with LukS-PV and one LukF-PV mutant (only slightly less for ΔS125-L128 and perhaps ΔI124-N126). The position of the oligomer, between 200 and 220 kDa, was also constant and consistent with a hexamer. Some faint intermediate bands (possibly dimers and trimers) were sometimes observed. Controls indicated that the native couple LukS-PV plus LukF-PV did not form oligomers in the absence of LUV. Only a faint band was noted in the pellet (Fig. 4B), probably due to some spontaneous aggregation in solution, as occurs with alpha-toxin (12).

For HlgA combinations instead, stable oligomers of about 200 kDa were detected only with LukF-PV ΔN123-G127, ΔI124-N126, and ΔS125-L128 and to a lesser extent with wt. In some cases, a small fraction of the material did not enter the separating gel, suggesting the presence of even larger aggregates.

DISCUSSION

In a previous work, mutations in the stem domain of LukF-PV were shown to generate a leucotoxin where the pore-forming ability was discoupled from Ca^{2+} entry (2). This new toxin failed also to induce rabbit skin dermonecrosis, demonstrating the importance of pore formation in PVL virulence. The inhibition of pore-forming activity could be due either to a destabilization of the final pore or to difficulties in its insertion, but in any case it did not prevent the formation of a still-uncharacterized intermediate that could open Ca^{2+} channels.

Another intriguing observation is that though F components are 70 to 80% identical, the HlgA plus HlgB couple is strongly hemolytic, whereas HlgA plus LukF-PV does not lyse RRBC. Therefore, one cannot exclude that fine arrangements between β-hairpins of heterologous subunits influence the final activity of leucotoxins.

Here, we used different membrane systems to investigate the compatibility for biological activity between the β-hairpins of three native class S proteins and those of LukF-PV and HlgB carrying different mutations. Deletions ranging from 3 to 6 amino acids (aa) were introduced at the extremity of the β-hairpin (Fig. 5), modeled according to references 19 and 22. In general, the shorter was the deletion, the more active was the mutant (Tables 1 and 2; Fig. 1). Each mutant retained significant binding but variable activity according to the combined S protein. Only the longest deletion, LukF-PV ΔI124-S129, had a reduced binding and no biological activity, whatever the combined class S component, despite the finding that oligomers could still be observed on PMNs (Fig. 4). This 6-aa deletion covers an important surface-exposed part of the folded stem in the water-soluble form of LukF-PV, including the end of β-strand ST2 and part of the loop joining it to ST3 (19). The loss of biological activity probably occurs because the remaining transmembrane β-hairpin is too short to span the membrane (Fig. 5). As the binding was also reduced (Table 1), it is possible that some conformational modifications occur even in the monomer. Similarly, the deletion of 25 residues from the stem domain of staphylococcal alpha-toxin still allowed its binding to membranes and even oligomerization but abolished its activity (3).

To the contrary, mutants with the shortest deletions of 3 aa (LukF-PV ΔS125-G127, LukF-PV ΔI124-N126, and LukF-PV ΔG127-S129) did not lose biological activity and were even more active than the wt in combination with HlgC. LukF-PV ΔI124-N126 and LukF-PV ΔG127-S129 (but not LukF-PV ΔS125-G127) showed only slightly diminished pore-forming activity in PMNs when combined with LukS-PV, but they caused normal Ca^{2+} entry. All were able to form oligomers on PMNs with every S component, on RRBC with HlgA, and on LUV with LukS-PV. These three mutants generated hemolysis of RRBC in association with either HlgA or HlgC (except for LukF-PV ΔI124-N126 and HlgC) and even HRBC were permeabilized by LukF-PV ΔS125-G127 with HlgA, whereby wt LukF-PV was inefficient (Fig. 3). These new results show that unilateral modification of the β-hairpin of one component of the leucotoxin couple could even enhance its activity. They indicate that 3-aa deletions still allowed the formation of β-hairpins long enough to form a stable pore (Fig. 5B). Such deletions could overcome a reduced ability to form the β-barrel with an easier unfolding of the stem. In fact, in the monomer, the stem domain is kept in place by interactions which must be broken to open the β-hairpin. A small deletion would decrease these interactions and could make the toxin even more efficient than the wt in assembling the β-barrel. The stabilizing interactions, occurring in the monomer, are most likely those between the hydrophobic couple I124 and V114 and the hydrogen bond formed between S125 and T113 (19).

The 4-aa deletion (LukF-PV ΔS125-L128) showed, with LukS-PV, a more pronounced discoupling of the two functions than the 3-aa deletions; meanwhile, in combination with HlgA it was almost as active as the wt, and with HlgC even more efficient. Oligomers were observed on PMNs, LUV, and RRBC. Although not permeabilizing purely lipidic membranes, this mutant hemolysed RRBC when combined with HlgA (Fig. 3). Therefore, this deletion also leaves a β-hairpin long enough to form a pore (Fig. 5A and B) and is more easily refolded, as demonstrated by the gain of biological activity on RRBC and PMNs with HlgA and HlgC.

The 5-aa deletion, LukF-PV ΔN123-G127, displayed instead a pore formation highly discoupled from Ca^{2+} channel activation. Combined with HlgA and to a lesser extent with HlgC, it had still hemolytic activity on RRBC (Fig. 3). All the combinations tested gathered oligomers on PMNs, RRBC, and LUV. Therefore, the deletion of 5 aa could still be tolerated by the β-barrel structure, though the β-hairpin formed is likely too short to form a truly stable pore (Fig. 5B). Nonetheless, the refolding of the stem from the monomer is apparently sufficient to produce a prepore able to activate Ca^{2+} channels.

The extent of discoupling between the pore-forming function and Ca^{2+} entry, observed with deletions of 4 or 5 aa, was dependent on the combined S component. With LukS-PV, the instability of the functional pore was observed with the deletion of LukF-PV residues located at the cytoplasmic extremity of the β-strands of the stem domain, i.e., N123, I124, L128, and S129. Instead, the absence of three polar residues, S125 to G127, improved pore formation, whatever the combined S component. Therefore, the presence of hydrophobic residues at the cytoplasmic side of the extended β-hairpins (e.g., I124 and L128) seems to be important for a better pore formation. Interestingly, the β-hairpins of HlgA and HlgC bear at the cytoplasmic side two hydrophobic residues more than that of LukS-PV, i.e., A118 and I121 of HlgA (or A120 and L123 of HlgC), in place of G118 and T121 of LukS-PV (Fig. 5A). This might help in the stabilization of pores with deletion mutants of LukF-PV having a reduced hydrophobicity.

Some point mutations in the stem were also investigated. The discoupling of Ca^{2+} induction from ethidium entry was previously described for LukF-PV G130D in combination with LukS-PV (2), whereas here a concerted decrease of both functions was observed with HlgA and a complete loss of biological activity with HlgC. However, it was possible to detect an oligomer on human PMNs with every combination. Recently, Gauduchon et al. (8) reported that LukS-PV and HlgC, but not HlgA, compete for their binding on human PMNs. Moreover, phorbol 12-myristyl 13-acetate treatment of human PMNs prevented the binding of LukS-PV, and this effect was blocked by staurosporin, an inhibitor of protein kinase C activation, suggesting that Ca^{2+} induction in target cells involves a membrane receptor which could bind both LukS-PV and HlgC. Since

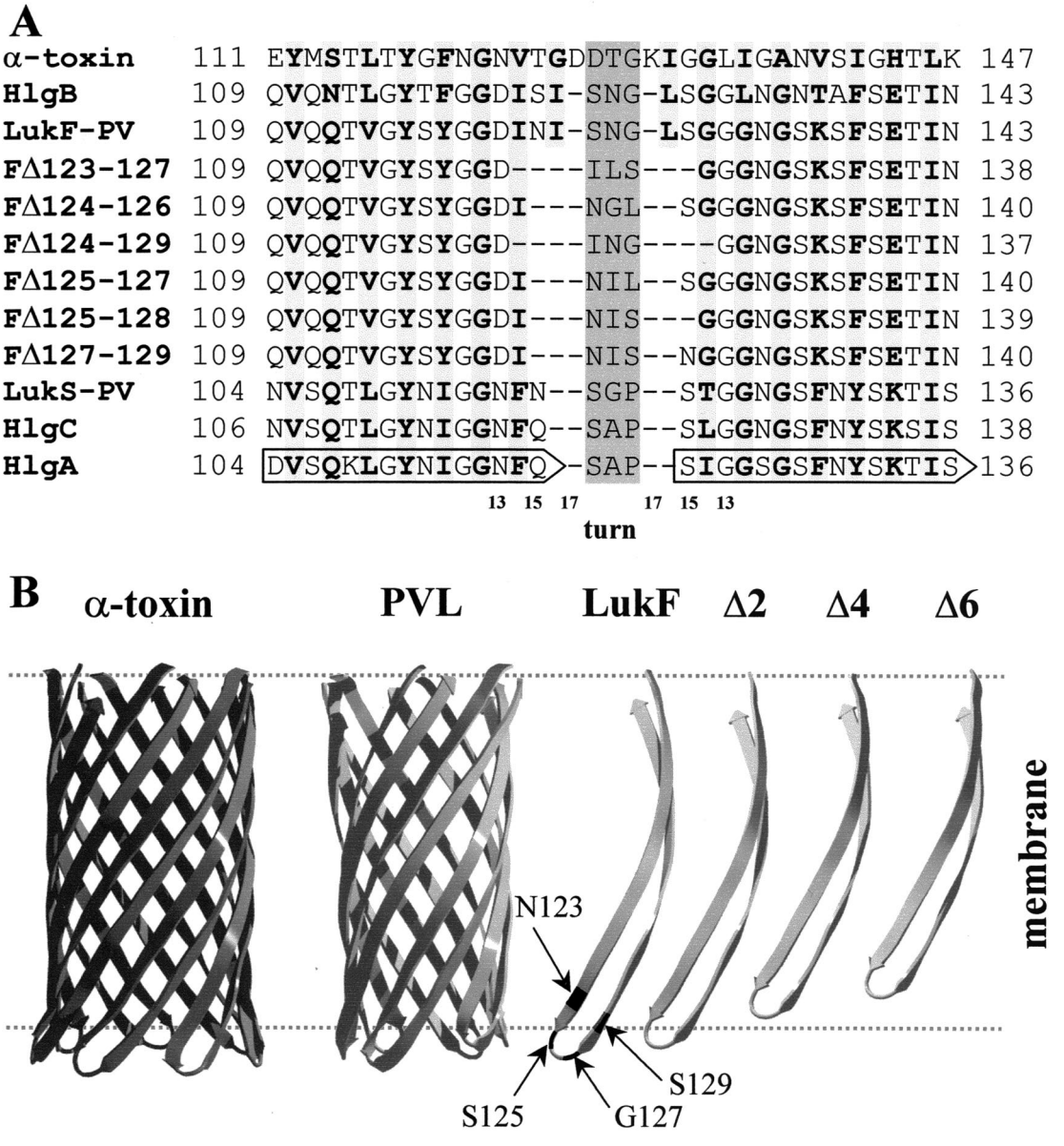

FIG. 5. Model of the structural organization of the β-hairpins of the S and F proteins of the leucotoxin pair compared to alpha-toxin. (A) The hairpin region forming the stem of alpha-toxin is aligned to corresponding regions of the wt bicomponent toxins (18) and the deletion mutants. Based on this alignment, the turn region of each component, either wt or mutated, was assigned as a central shaded triplet of residues. The length of the strands forming the stem in the wt toxins varies between 15 and 17 residues, whereas it is from 13 to 15 aa in the deletion mutants, as indicated by the scale below the sequences. Strand residues facing the side of the membrane are in bold over lightly shaded background. Numbering is according to the leucotoxin components (GenBank-EMBL databank accession numbers X72700 for LukS-PV and LukF-PV; X81586 for HlgA, HlgC, and HlgB). (B) The structure of the β-barrel stem of alpha-toxin (21) is compared to a model of that of leucotoxins generated with the program Deep View (http://www.expasy.ch/spdbv/) (11) and adapted from reference 19. Despite strands of the latter being one or two residues shorter, the β-barrel has approximately the same length as that of alpha-toxin because of a smaller angle with respect to the pore axis. An isolated β-hairpin of LukF-PV (or HlgB) is shown to the right. Positions 123, 125, 127, and 129 are highlighted. Next to it are β-hairpins shorter by two (corresponding to the length of the S-components LukS-PV, HlgA, or HlgC), four (ΔS125-L128), or six residues (ΔI124-S129). Other deletion mutants are intermediate between the strands Δ2 and Δ6, e.g., LukF-PV ΔN123-G127. The approximate position of the lipid bilayer is indicated by dashed lines. Hairpins shorter than Δ4 are not long enough to span the membrane.

oligomers of apparent molecular mass similar to the wt were detected when LukF-PV G130D was combined with either LukS-PV or HlgC, but Ca^{2+} entry was only observed with LukS-PV, it seems likely that Ca^{2+} induction is allowed by an intermediate occurring after oligomerization. Such oligomers should form very rapidly, since Ca^{2+} entry occurs within 100 s from leucotoxin application (23), a clear difference from the slowly assembling oligomers of perfringolysin O (13). This activation may depend on further interactions between stem domains of S and F components, which are not fulfilled in the case of HlgC plus LukF-PV G130D. In comparison, HlgB G130D did not generate any discoupling, but rather a concerted decrease of the two functions whatever the class S protein combined. In fact, when considering the β-hairpin se-

quences of LukF-PV and HlgB (Fig. 5A), the latter has two more hydrophobic residues (F118 and L132 instead of Y118 and G132) that are presumably oriented towards the membrane. This presence might help the dynamics of the β-hairpin insertion and may contribute to a better stabilization of the functional pore, partially compensating for the Asp substitution in HlgB.

Two other point mutations, S129A and G131D, had less or no impact on the biological activity of LukF-PV. Only a reduced pore formation, producing a substantial discoupling, was recorded with LukF-PV G131D in combination with either LukS-PV or HlgC. As a matter of fact, these two positions should face the pore lumen, thus being less critical.

In conclusion, our results about staphylococcal leucotoxin assembly support the concept of the existence of a prepore (14, 25). Ca^{2+} influx may result from the formation of a structural intermediate, which follows the aggregation of the oligomer but is not yet a functional pore. The lag time between the beginning of Ca^{2+} induction and the entry of ethidium through the pore can last even a few minutes. Pore formation depends both on the given S/F combination and on membrane composition. Indeed, none of these mutants, including combinations that were hemolytic, could permeabilize PC-Cho synthetic membranes (LUV), despite the formation of oligomers achieved by most of the tested combinations. Therefore, the presence of specific membrane ligands, favoring the stabilization of the pore or the dynamics of unfolding and insertion of the β-hairpins, may be required. Similarly, alpha-hemolysin does not form the pore through the membrane of resistant cells even if it oligomerizes (26), and it has a preference for synthetic lipid bilayers containing choline-type phospholipids and cholesterol rather than those containing other phospho- or sphingoglycolipids (4, 6).

We can also conclude that the small region located in the loop of the β-hairpins largely influences the functional pore configuration and may be implicated in a series of interactions during stem refolding and insertion of the β-barrel. Further studies will be required to fully describe the interactions between β-hairpins and between residues of leucotoxins and membrane compounds.

ACKNOWLEDGMENTS

We are grateful to D. Keller, R. Girardot, and J. Voegelin for their skillful technical assistance and to M. Dalla Serra and Lionel Mourey for help in computer modeling.

This work was supported by the research fund of the Institut de Bactériologie de la Faculté de Médecine de Strasbourg, by grant EA-1318 from the Direction de la Recherche et des Etudes Doctorales (DRED), Ministère de la Recherche, des Sciences et de la Technologie, and by structural funds of the Consiglio Nazionale delle Ricerche (CNR).

REFERENCES

1. **Alouf, J. E., and J. H. Freer (ed.)** 1999. The comprehensive sourcebook of bacterial protein toxins, 2nd ed. Academic Press, London, United Kingdom.
2. **Baba-Moussa, L., S. Werner, D. A. Colin, L. Mourey, J.-D. Pédelacq, J. P. Samama, A. Sanni, H. Monteil, and G. Prévost.** 1999. Discoupling the Ca^{2+}-activation from the pore-forming function of the bi-component Panton-Valentine leucocidin in human PMNs. FEBS Lett. **461:**280–286.
3. **Cheley, S., G. Braha, X. F. Lu, S. Conlan, and H. Bayley.** 1999. A functional protein pore with a "retro" transmembrane domain. Protein Sci. **8:**1257–1267.
4. **Cheley, S., M. S. Malghani, L. Z. Song, M. Hobaugh, J. E. Gouaux, J. Yang, and H. Bayley.** 1997. Spontaneous oligomerization of a staphylococcal alpha-hemolysin conformationally constrained by removal of residues that form the transmembrane beta-barrel. Protein Eng. **10:**1433–1443.
5. **Ferreras, M., F. Höper, M. Dalla Serra, D. A. Colin, G. Prévost, and G. Menestrina.** 1998. The interaction of *Staphylococcus aureus* bi-component gamma hemolysins and leucocidins with cells and model membranes. Biochim. Biophys. Acta **1414:**108–126.
6. **Forti, S., and G. Menestrina.** 1989. Staphylococcal alpha-toxin increases the permeability of lipid vesicles by a cholesterol and pH dependent assembly of oligomeric channels. Eur. J. Biochem. **181:**767–773.
7. **Gauduchon, V., J. Reutenauer, S. Werner, G. Prévost, H. Monteil, and D. A. Colin.** 2000. The panton valentine leukocidin binding on human polymorphonuclear neutrophils. Med. Microbiol. Immunol. **189:**36.
8. **Gauduchon, V., S. Werner, G. Prévost, H. Monteil, and D. A. Colin.** 2001. Flow cytometric determination of Panton-Valentine leucocidin S component binding. Infect. Immun. **69:**2390–2395.
9. **Gouaux, J. E.** 1998. Alpha-hemolysin from *Staphylococcus aureus*: an archetype of beta-barrel, channel-forming toxins. J. Struct. Biol. **121:**110–122.
10. **Gravet, A., D. A. Colin, D. Keller, R. Girardot, H. Monteil, and G. Prévost.** 1998. Characterization of a novel structural member, LukE-LukD, of the bi-component staphylococcal leucotoxins family. FEBS Lett. **436:**202–208.
11. **Guex, N., and M. C. Peitsch.** 1997. SWISS-MODEL and the Swiss-Pdb Viewer: an environment for comparative protein modeling. Electrophoresis **18:**2714–2723.
12. **Harshman, S., N. Sugg, B. Gametchu, and R. W. Harrison.** 1986. Staphylococcal alpha-toxin: a structure-function study using a monoclonal antibody. Toxicon **24:**403–411.
13. **Hotze, E. M., E. M. Wilson-Kubalek, J. Rossjohn, M. W. Parker, A. E. Johnson, and R. K. Tweten.** 2001. Arresting pore formation of a cholesterol-dependent cytolysin by disulfide trapping synchronizes the insertion of the transmembrane beta-sheet from a prepore intermediate. J. Biol. Chem. **276:**8261–8268.
14. **Lesieur, C., B. Vécsey-Semjén, L. Abrami, M. Fivaz, and F. G. van der Goot.** 1997. Membrane insertion: the strategies of toxins. Mol. Membr. Biol. **14:**45–64.
15. **Menestrina, G., M. Dalla Serra, and G. Prévost.** 2001. Mode of action of β-barrel pore-forming toxins of the staphylococcal α-toxin family. Toxicon **39:**1661–1672.
16. **Meunier, O., A. Falkenrodt, H. Monteil, and D. A. Colin.** 1995. Application of flow cytometry in toxinology: pathophysiology of human polymorphonuclear leukocytes damaged by a pore-forming toxin from *Staphylococcus aureus*. Cytometry **21:**241–247.
17. **Meunier, O., M. Ferreras, G. Supersac, F. Höper, L. Baba-Moussa, H. Monteil, D. A. Colin, G. Menestrina, and G. Prévost.** 1997. A predicted β-sheet from class S components of staphylococcal gamma-hemolysins is essential for the secondary interaction of the class F component. Biochim. Biophys. Acta **1326:**275–286.
18. **Olson, R., H. Nariya, K. Yokota, Y. Kamio, and J. E. Gouaux.** 1999. Crystal structure of staphylococcal LukF delineates conformational changes accompanying formation of transmembrane channel. Nat. Struct. Biol. **6:**134–140.
19. **Pédelacq, J.-D., L. Maveyraud, G. Prévost, L. Baba-Moussa, A. Gonzalez, E. Courcelle, W. Shepard, H. Monteil, J.-P. Samama, and L. Mourey.** 1999. The structure of a *Staphylococcus aureus* leucocidin component (LukF-PV) reveals the fold of the water-soluble species of a family of transmembrane pore-forming toxins. Structure **7:**277–287.
20. **Prévost, G., B. Cribier, P. Couppié, P. Petiau, G. Supersac, V. Finck-Barbançon, H. Monteil, and Y. Piémont.** 1995. Panton-Valentine leucocidin and gamma-hemolysin from *Staphylococcus aureus* ATCC 49775 are encoded by distinct genetic loci and have different biological activities. Infect. Immun. **63:**4121–4129.
21. **Prévost, G., L. Mourey, D. A. Colin, and G. Menestrina.** 2001. Staphylococcal pore-forming toxins. Curr. Top. Microbiol. Immunol. **257:**53–83.
22. **Song, L., M. R. Hobaugh, C. Shustak, S. Cheley, H. Bayley, and J. E. Gouaux.** 1996. Structure of staphylococcal alpha-hemolysin, a heptameric transmembrane pore. Science **274:**1859–1866.
23. **Staali, L., H. Monteil, and D. A. Colin.** 1998. The staphylococcal pore-forming leukotoxins open Ca^{2+} channels in the membrane of human polymorphonuclear neutrophils. J. Membr. Biol. **162:**209–216.
24. **Tejuca, M., M. Dalla Serra, M. Ferreras, M. E. Lanio, and G. Menestrina.** 1996. The mechanism of membrane permeabilisation by sticholysin I, a cytolysin isolated from the venom of the sea anemone *Stichodactyla helianthus*. Biochemistry **35:**14947–14957.
25. **Valeva, A., M. Palmer, and S. Bhakdi.** 1997. Staphylococcal alpha-toxin: formation of the heptameric pore is partially cooperative and proceeds through multiple intermediate stages. Biochemistry **36:**13298–13304.
26. **Valeva, A., I. Walev, M. Pinkernell, B. Walker, H. Bayley, M. Palmer, and S. Bhakdi.** 1997. Transmembrane beta-barrel of staphylococcal alpha-toxin forms in sensitive but not in resistant cells. Proc. Natl. Acad. Sci. USA **94:**11607–11611.

Editor: J. T. Barbieri